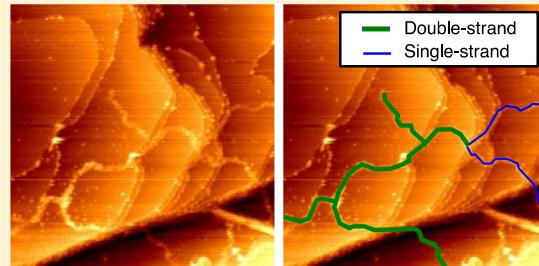


# Structural Modification of DNA Studied by Scanning Tunneling Microscopy

Kohei Terasaki and Takashi Yokoyama\*

Department of Nanoscience and Technology, Yokohama City University, 22-2 Seto 236-0027, Japan

**ABSTRACT:** In addition to the well-known double-helix structure of deoxyribonucleic acid (DNA), theoretical simulations have predicted structural variants, such as cross and T-shaped formations. The direct visualization of individual DNA molecules by scanning probe microscopy should be able to identify these structures. In this study, we examine various structures of DNA deposited on Au(111) by using an electrospray method and analyzing with a low-temperature scanning tunneling microscope. We could identify in detail several interesting structures. In particular, we found that double-stranded DNAs are partially unraveled into single-stranded DNAs and we confirmed the presence of T-shaped DNA structures.



## INTRODUCTION

Deoxyribonucleic acid (DNA) is a large polymeric molecule, which is a molecule essential for life. It is involved in inheritance and expression of genetic information. The three-dimensional structure of DNA has been determined at atomic resolution by X-ray crystallography<sup>1</sup> and nuclear magnetic resonance.<sup>2,3</sup> In general, the double-stranded structure of DNA is composed of two polynucleotides (single-stranded DNAs), forming the double-helix structure. In addition, theoretical simulations have shown structural modifications of DNA, such as cross and T-shaped structures.<sup>4</sup> In order to identify them, it is necessary to clarify differences in the structures of individual DNAs. However, they cannot be clarified by X-ray crystallography and nuclear magnetic resonance because these methods determine an average structure of DNA.

Scanning probe microscopy (SPM) is a method of structural analysis, which enables us to visualize the adsorbed molecules on a surface at the single molecular level. Among SPM, scanning tunneling microscopy (STM) and atomic force microscopy (AFM) are able to image single molecules with high resolution. With these techniques, linear and circular DNAs, as well as the double-helix structures, have been observed under the atmosphere or vacuum conditions, or in the aqueous solution.<sup>5–10</sup> Although intact DNAs have been reported in most cases, branched DNA has been observed by AFM under vacuum.<sup>11</sup> Nevertheless, the detailed structures were not clear because of insufficient resolution. Because STM tends to achieve higher resolution than AFM, especially under vacuum and at low temperature, STM should be an effective method to show structural modification of individual DNAs in more detail.

For the STM observation under vacuum, DNA must be deposited on a surface in vacuum. Nevertheless, DNA cannot be thermally sublimated, and thus, it is usually difficult to be deposited on surfaces in vacuum. Electrospray ionization has been widely used to introduce biomolecules into vacuum for

mass spectrometry.<sup>12</sup> This technique has been recently utilized as a molecular ion source for molecular deposition in vacuum.<sup>13–17</sup> Using the electrospray method, we have previously deposited oligothiophene wires with lengths from 10 to 120 nm on Au(111) and identified molecular shapes from high-resolution STM images.<sup>17</sup>

Here, we deposit DNA onto a single-crystal surface of Au(111) by using the electrospray method, and detailed shapes of deposited DNA are directly visualized by STM under ultrahigh vacuum (UHV) condition at 78 K. From the STM images, we find partially formed single-stranded DNAs as well as double-stranded DNAs. Various shapes of DNAs, such as folded and T-shaped DNA, are also observed.

## EXPERIMENTAL METHODS

We used a linear DNA molecule, Lambda *Hind* III digest, purchased from Takara Bio Corp. (Shiga, JPN). It has eight kinds of DNA fragments with different number of base pairs (A–H). The relative number of base pairs was 23130, 9416, 6557, 4361, 2322, 2027, 564, and 125. The concentration of DNA was 0.5  $\mu\text{g}/\mu\text{L}$  in the original buffer solution of 10 mM Tris-HCl and 1 mM ethylenediaminetetraacetic acid. The DNA solution was diluted 10 times in water and volatile acetonitrile (the mixing solvent ratio of 1:1). The final concentration of DNA was  $4.6 \times 10^{-2} \mu\text{g}/\mu\text{L}$ .

Molecular deposition was performed using the electrospray deposition system.<sup>17</sup> The electrospray ion of DNA was produced at ambient pressure by applying a high electric field (typically 2.2–2.5 kV) to a small flow of the DNA solution in the needle tube. The DNA solution was supplied to the needle tube using a controlled syringe pump at a constant

Received: December 17, 2018

Revised: January 30, 2019

Published: February 5, 2019

flow rate of  $2.0 \mu\text{L}/\text{min}$ . At the tip of the needle tube, the applied high electric field results in the formation of highly charged liquid droplets, followed by droplet shrinkage through the Coulomb explosion and solvent evaporation. The generated gas-phase ions were introduced to the first vacuum chamber through an entrance capillary and guided to the UHV deposition chamber via four differential pumping stages.<sup>17</sup> In the deposition chamber, the pressure was maintained at less than  $1 \times 10^{-5} \text{ Pa}$  during deposition, whereas the base pressure was less than  $5 \times 10^{-7} \text{ Pa}$ .

A clean Au(111) surface, used as the substrate, was prepared by repeated cycles of  $\text{Ar}^+$  sputtering and annealing. The DNA deposition onto the Au(111) surface was achieved by the exposure to the DNA ion beams in the deposition chamber at room temperature and then the sample was kept for 60 min without the ion exposure in UHV to desorb the residual solvent molecules.<sup>17</sup> After repeated cycles (2–8 times) of the 5 min deposition and 60 min without deposition, the sample was subsequently transferred to the low-temperature STM stage without thermal annealing. All STM images were acquired in a constant current mode of 50 pA at 78 K under UHV condition (less than  $5 \times 10^{-9} \text{ Pa}$ ).

## RESULTS AND DISCUSSION

**Figure 1** shows an STM image of the Au(111) surface after the deposition of linear DNA by using the electrospray method, in

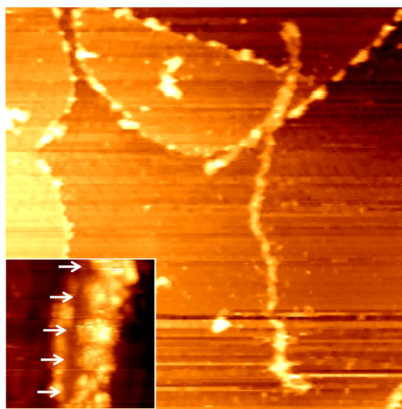


**Figure 1.** STM image ( $V_s = 4.0 \text{ V}; I_t = 50 \text{ pA}$ ;  $200 \text{ nm} \times 200 \text{ nm}$ ) of a linear DNA deposited on Au(111) using an electrospray method, which is extended to 190 nm in length and 6 nm in width. Inset: High-resolution STM image ( $V_s = 4.0 \text{ V}; I_t = 50 \text{ pA}$ ;  $20 \text{ nm} \times 20 \text{ nm}$ ) of the linear DNA, in which the periodic structures as indicated by white arrows are clearly observed with a periodicity of  $4.5 \pm 0.2 \text{ nm}$ .

which a bright string of DNA appears to be extended of 190 nm in length and 6 nm in width. Although the width of the DNA is known to be about 2 nm,<sup>18</sup> the apparent width of 6 nm in **Figure 1** is wider than that. Such a wider width (about 3–6 nm) has been observed by SPM (AFM and STM).<sup>5–10</sup> In general, the SPM tip is noncontact with a sample surface during scanning, and thus, the apparent width of the sample imaged by SPM could be wider than its actual width. The inset of **Figure 1** shows the high-resolution STM image of DNA, which is composed of periodic bright protrusions with a periodicity of  $4.5 \pm 0.2 \text{ nm}$ , indicating the double helix of DNA. The periodicity of the double helix has been reported to be about 3 nm,<sup>18</sup> and the periodicity of 2.6–3.8 nm has been observed by AFM and STM.<sup>7,8,10</sup> As the periodicity we obtained, of 4.5 nm, is slightly longer than previous estimates,

the deposited DNA shown in **Figure 1** may be structurally relaxed because of the molecule–surface interactions.

In contrast to the straight DNA, **Figure 2a** shows an STM image of another DNA shape. We find that the apparent width

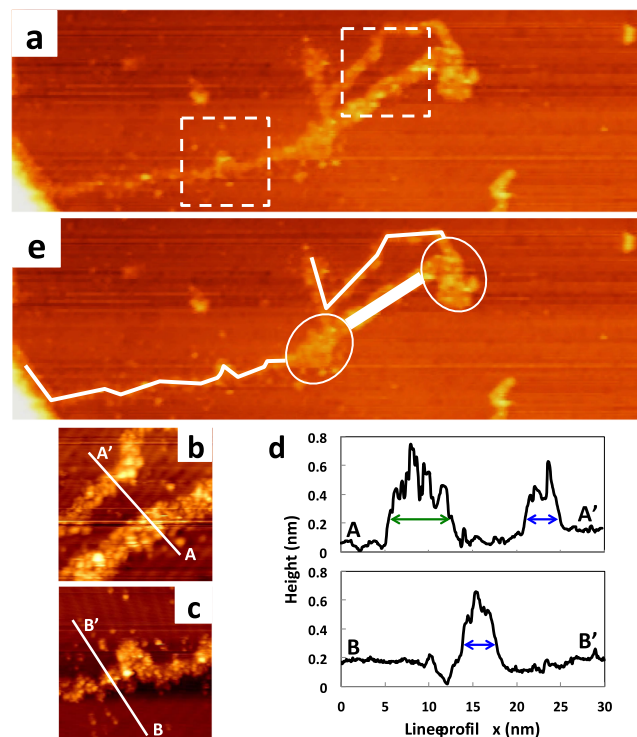


**Figure 2.** Double-stranded DNA separated into single-stranded DNA on Au(111). (a) Large-area STM image ( $V_s = 3.5 \text{ V}; I_t = 50 \text{ pA}$ ;  $80 \times 250 \text{ nm}$ ) of a different-shaped DNA in contrast to straight-shaped DNA. (b,c) High-resolution STM images ( $V_s = 4.0 \text{ V}; I_t = 50 \text{ pA}$  for (b),  $V_s = 3.5 \text{ V}; I_t = 50 \text{ pA}$  for (c)) of the white dotted square regions of (a). The DNA has wide and narrow widths. (d) Cross-sectional profiles along the white line A–A' in (b) and the white line B–B' in (c), in which the wide and narrow apparent widths are 6 and 3 nm, respectively. (e) Same image as (a), in which the DNA is differentiated as double-stranded DNA (thick line) from single-stranded DNA (thin line) by width. Nevertheless, the detail of white circle region is not clear.

of the DNA depends on the position as indicated in the cross-sectional profiles (see **Figure 2d**) measured along the A–A' and B–B' lines in **Figure 2b,c**, respectively. The measured widths are about 6 and 3 nm as indicated by green and blue arrows in **Figure 2d**, respectively. The apparent width of 6 nm might correspond with that of the double helix of DNA. On the other hand, the width of 3 nm is half of that. On the basis of the double helix of DNA being composed of two polynucleotide strands, the narrow width may correspond to single-stranded DNA. In **Figure 2e**, thin and thick lines, corresponding to the widths of 3 and 6 nm, respectively, are superimposed in the STM image. This indicates that the single-stranded DNA (thin line in **Figure 2e**) and the double-stranded DNA (thick line in **Figure 2e**) are presented simultaneously, even though only the double-stranded DNAs were deposited on the Au(111) surface.

As shown in **Figure 3a**, we also find a branched DNA. Such a branched DNA has been reported by AFM studies,<sup>11</sup> although the detailed structures have not been fully investigated because of the insufficient resolution. In the branched DNA observed

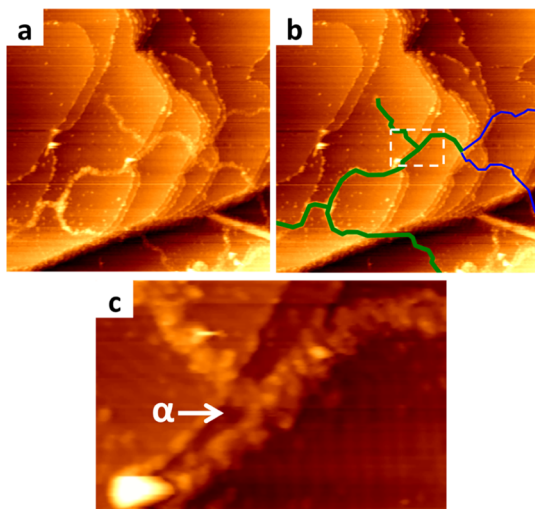


**Figure 3.** Branched DNA on Au(111). (a) Large-area STM image ( $V_s = 4.0$  V;  $I_t = 50$  pA;  $300$  nm  $\times$   $300$  nm) of a branched DNA, which has three branch points. (b) Same image as (a), in which the DNA is marked as double-stranded DNA (green) from single-stranded DNA (blue) by width. (c) High-resolution STM image ( $V_s = 4.0$  V;  $I_t = 50$  pA;  $40$  nm  $\times$   $60$  nm) of the white dotted rectangle region of (b), in which three DNAs are connected at the  $\alpha$  point forming T-shaped DNA.

here, the apparent widths are different depending on the branches, as marked by colored lines in Figure 3b. The green and blue lines indicate the widths of 6 and 3 nm, respectively. On right side in Figure 3b, a branch point appears to be composed of a double-stranded DNA and two single-stranded DNAs. Thus, the double-stranded DNA seems to open into two single-stranded DNAs. In contrast, at other branch points, all measured widths of the DNA are almost identical to 6 nm (shown as green lines). Figure 3c is a magnified image of the branch area indicated by the white dotted rectangle in Figure 3b. Although the detail of the branch structure is not clear from this, the branch appears to be composed of double-stranded DNA, in which three DNAs are connected at the point indicated by the white arrow. This structure may correspond to the three terminal contact of the double-strand DNA, which has been predicted by theoretical simulations<sup>4</sup> and called T-shaped DNA.

Besides the extended DNAs shown in Figures 1–3, we also observe the folded (or looped) DNA in Figure 4a. According to the cross-sectional profile measured along the A–A' line shown in Figure 4b, the width is about 1.5 nm, which is almost constant all along the folded DNA. Because of the narrower width, the folded structure in Figure 4 may be composed of a single-stranded DNA. This indicates that the double-stranded DNA is completely separated into a single-stranded DNA. Compared with the single strand width of 3 nm in Figures 2 and 3, the narrow width of 1.5 nm should be caused by the tip shape effect. In general, the single-stranded DNA tends to fold back on itself, forming loops. So far, the single-stranded DNAs have been observed by AFM,<sup>9,19</sup> which tend to be folded on mica. In a similar fashion, the DNA in Figure 4 is folded on Au(111), which shows the foldability of the single-stranded DNA. Coil structures of DNA have been reported, and these have been interpreted as rings-on-a-string conformations analyzed using a polyelectrolyte chain in poor solvent.<sup>20–22</sup>

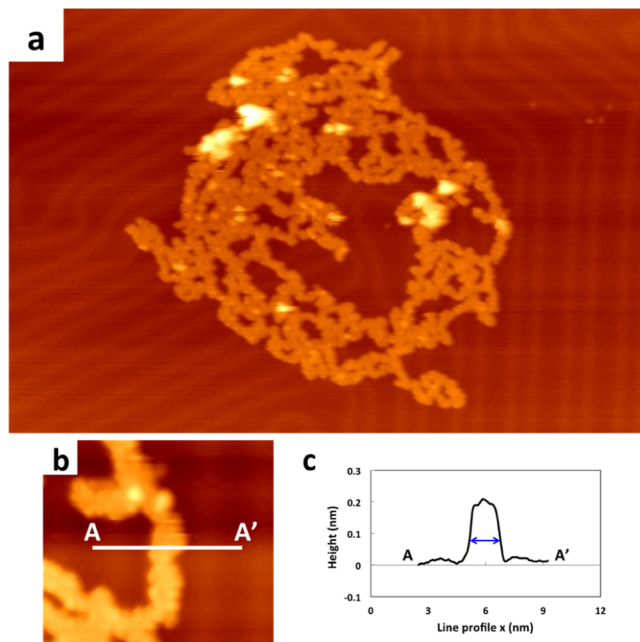


**Figure 4.** Folded (or looped) DNA on Au(111). (a) Large-area STM image ( $V_s = -3.0$  V;  $I_t = 50$  pA;  $50$  nm  $\times$   $75$  nm) of a folded DNA. (b) Small-area STM image ( $V_s = -3.5$  V;  $I_t = 50$  pA;  $9.0$  nm  $\times$   $10.0$  nm) of (a). (c) Cross-sectional profile along the white line A–A' in (b). All width (about 1.5 nm) of the DNA is smaller than that of double-strand *in vivo* (2.0 nm).

## CONCLUSIONS

In this study, the various shapes of DNA were identified by STM. From 91 DNA molecules tested, we have observed linear DNA and branched DNA with the abundance ratio of 89.0 and 11.0%, respectively. In addition, we found that linear DNA includes double-stranded DNA and single-stranded DNA. Branched DNA includes the partially formed single-stranded DNA, T-shaped DNA, and their mixtures. The relative abundance ratios were 56.0, 33.0, 5.5, 4.4, and 1.1%, respectively. This indicates that about half of the adsorbed DNAs have changed to structures different from the double-helix structure of DNA.

On the other hand, the majority of linear DNAs are less than 200 nm in length, and the lengths of 40–50 nm were most abundant. In general, one periodicity of the double helix is composed of about 10 base pairs, corresponding to the length of around 3.4 nm. The Lambda Hind III digest molecules that we used has Fragment A–H, in which the relative lengths, roughly estimated from the number of base pairs, are 7864.2, 3201.4, 2229.4, 1482.7, 789.5, 689.2, 191.8, and 42.5 nm for A–H, respectively. Thus, this can explain the abundance of 40–50 nm DNA segments because Fragment H with the length of 42.5 nm should be mainly adsorbed on the Au(111) surface. The linear DNAs longer than 200 nm may be fragmented during the deposition or cannot be ionized.

We have performed the vacuum deposition of linear DNA onto Au(111) using the electrospray method. Various shapes of DNA were identified using LT-STM in the UHV condition, which were linear DNA (double-stranded DNA and single-stranded DNA) and branched DNA. The latter was a mixture of single-stranded DNA and T-shaped DNA observed for the first time. On the other hand, we found that the linear DNAs longer than 200 nm may be mainly fragmented or cannot be

ionized, and thus we suspected that the electrospray method used may induce chemical modification to the DNA.<sup>23</sup> Furthermore, we used a large quantity of acetonitrile (an organic solvent) that has low affinity with DNA in addition to water. Therefore, the electrospray ionization with the organic solvent could be the cause of fragmentation and structural modification of the DNA.<sup>23–26</sup>

## AUTHOR INFORMATION

### Corresponding Author

\*E-mail: [tyoko@yokohama-cu.ac.jp](mailto:tyoko@yokohama-cu.ac.jp). Phone/Fax: +81 (0)45 787 2160.

### ORCID

Takashi Yokoyama: [0000-0002-5410-5030](https://orcid.org/0000-0002-5410-5030)

### Funding

This work was financially supported by grants-in-aid for scientific research from Japan Society for the Promotion of Science. We would like to thank Prof. R. Micheletto for his critical reading of our manuscript.

### Notes

The authors declare no competing financial interest.

## REFERENCES

- (1) Mooers, B. H. M. Crystallographic Studies of DNA and RNA. *Methods* **2009**, *47*, 168–176.
- (2) Shajani, Z.; Varani, G. NMR Studies of Dynamics in RNA and DNA by <sup>13</sup>C Relaxation. *Biopolymers* **2007**, *86*, 348–359.
- (3) Zídek, L.; Štefl, R.; Sklenář, V. NMR Methodology for the Study of Nucleic Acids. *Curr. Opin. Struct. Biol.* **2001**, *11*, 275–281.
- (4) Doye, J. P. K.; Ouldridge, T. E.; Louis, A. A.; Romano, F.; Šulc, P.; Matek, C.; Snodin, B. E. K.; Rovigatti, L.; Schreck, J. S.; Harrison, R. M.; et al. Coarse-Graining DNA for Simulations of DNA Nanotechnology. *Phys. Chem. Chem. Phys.* **2013**, *15*, 20395–20414.
- (5) Hansma, H. G.; Vesenka, J.; Siegerist, C.; Kelderman, G.; Morrett, H.; Sinsheimer, R. L.; Elings, V.; Bustamante, C.; Hansma, P. K. Reproducible Imaging and Dissection of Plasmid DNA Under Liquid with the Atomic Force Microscope. *Science* **1992**, *256*, 1180–1184.
- (6) Guckenberger, R.; Heim, M.; Cevc, G.; Knapp, H.; Wiegrabe, W.; Hillebrand, A. Scanning Tunneling Microscopy of Insulators and Biological Specimens Based on Lateral Conductivity of Ultrathin Water Films. *Science* **1994**, *266*, 1538–1540.
- (7) Mou, J.; Czajkowsky, D. M.; Zhang, Y.; Shao, Z. High-resolution atomic-force microscopy of DNA: the pitch of the double helix. *FEBS Lett.* **1995**, *371*, 279–282.
- (8) Tanaka, H.; Hamai, C.; Kanno, T.; Kawai, T. High-Resolution Scanning Tunneling Microscopy Imaging of DNA Molecules on Cu(111) Surfaces. *Surf. Sci.* **1999**, *432*, L611–L616.
- (9) Adamcik, J.; Klinov, D. V.; Witz, G.; Sekatskii, S. K.; Dietler, G. Observation of Single-Stranded DNA on Mica and Highly Oriented Pyrolytic Graphite by Atomic Force Microscopy. *FEBS Lett.* **2006**, *580*, 5671–5675.
- (10) Ido, S.; Kimura, K.; Oyabu, N.; Kobayashi, K.; Tsukada, M.; Matsushige, K.; Yamada, H. Beyond the Helix Pitch: Direct Visualization of Native DNA in Aqueous Solution. *ACS Nano* **2013**, *7*, 1817–1822.
- (11) Davies, E.; Teng, K. S.; Conlan, R. S.; Wilks, S. P. Ultra-High Resolution Imaging of DNA and Nucleosomes Using Non-Contact Atomic Force Microscopy. *FEBS Lett.* **2005**, *579*, 1702–1706.
- (12) Smith, R. D.; Loo, J. A.; Edmonds, C. G.; Barinaga, C. J.; Udseth, H. R. New Developments in Biochemical Mass Spectrometry: Electrospray Ionization. *Anal. Chem.* **1990**, *62*, 882–899.
- (13) Swarbrick, J. C.; Taylor, J. B.; O'Shea, J. N. Electrospray Deposition in Vacuum. *Appl. Surf. Sci.* **2006**, *252*, 5622–5626.
- (14) Rauschenbach, S.; Vogelgesang, R.; Malinowski, N.; Gerlach, J. W.; Benyoucef, M.; Costantini, G.; Deng, Z.; Thontasen, N.; Kern, K. Electrospray Ion Beam Deposition: Soft-Landing and Fragmentation of Functional Molecules at Solid Surfaces. *ACS Nano* **2009**, *3*, 2901–2910.
- (15) Hamann, C.; Wolmann, R.; Hong, I.-P.; Hauptmann, N.; Karan, S.; Berndt, R. Ultrahigh Vacuum Deposition of Organic Molecules by Electrospray Ionization. *Rev. Sci. Instrum.* **2011**, *82*, 033903.
- (16) O'Sullivan, M. C.; Sprafke, J. K.; Kondratuk, D. V.; Rinfray, C.; Claridge, T. D. W.; Saywell, A.; Blunt, M. O.; O'Shea, J. N.; Beton, P. H.; Malfois, M.; Anderson, H. L. Vernier Templating and Synthesis of a 12-Porphyrin Nano-Ring. *Nature* **2011**, *469*, 72–75.
- (17) Yokoyama, T.; Kogure, Y.; Kawasaki, M.; Tanaka, S.; Aoshima, K. Scanning Tunneling Microscopy Imaging of Long Oligothiophene Wires Deposited on Au(111) Using Electrospray Ionization. *J. Phys. Chem. C* **2013**, *117*, 18484–18487.
- (18) Marini, M.; Falqui, A.; Moretti, M.; Limongi, T.; Allione, M.; Genovese, A.; Lopatin, S.; Tirinato, L.; Das, G.; Torre, B.; Giugni, A.; Gentile, F.; Candeloro, P.; Di Fabrizio, E. The structure of DNA by direct imaging. *Sci. Adv.* **2015**, *1*, No. E1500734.
- (19) Hansma, H. G.; Revenko, I.; Kim, K.; Laney, D. E. Atomic Force Microscopy of Long and Short Double-Stranded, Single-Stranded and Triple-Stranded Nucleic Acids. *Nucleic Acids Res.* **1996**, *24*, 713–720.
- (20) Miyazawa, N.; Sakaue, T.; Yoshikawa, K.; Zana, R. Rings-on-a-string chain structure in DNA. *J. Chem. Phys.* **2005**, *122*, 044902.
- (21) Sakaue, T.; Yoshikawa, K. On the formation of rings-on-a-string conformations in a single polyelectrolyte chain: A possible scenario. *J. Chem. Phys.* **2006**, *125*, 074904.
- (22) Pereira, G. G. Charged, semi-flexible polymers under incompatible solvent conditions. *Curr. Appl. Phys.* **2008**, *8*, 347–350.
- (23) Shlyapnikov, Y. M.; Shlyapnikova, E. A.; Morozov, V. N. Reversible and Irreversible Mechanical Damaging of Large Double-Stranded DNA upon Electrospraying. *Anal. Chem.* **2016**, *88*, 7295–7301.
- (24) Fang, Y.; Hoh, J. H.; Spisz, T. S. Ethanol-Induced Structural Transitions of DNA on Mica. *Nucleic Acids Res.* **1999**, *27*, 1943–1949.
- (25) Pereira, G. G.; Williams, D. R. M. Toroidal Condensates of Semiflexible Polymers in Poor Solvents: Adsorption, Stretching, and Compression. *Biophys. J.* **2001**, *80*, 161–168.
- (26) Montesi, A.; Pasquali, M.; MacKintosh, F. C. Collapse of a semiflexible polymer in poor solvent. *Phys. Rev. E: Stat. Nonlin. Soft Matter Phys.* **2004**, *69*, 021916.